Isospin equilibration in neutron star mergers

Mark G. Alford [1,*] Alexander Haber [1,†] and Ziyuan Zhang [1,2,‡]

[1]*Physics Department, Washington University in Saint Louis, Saint Louis, Missouri 63130, USA*

[2]*McDonnell Center for the Space Sciences, Washington University in Saint Louis, Saint Louis, Missouri 63130, USA*

(Received 25 August 2023; revised 21 November 2023; accepted 28 March 2024; published 8 May 2024)

We analyze the isospin equilibration properties of neutrinoless nuclear (npe) matter in the temperature and density range that is relevant to neutron star mergers. Our analysis incorporates neutrino-transparency corrections to the isospin ("beta") equilibrium condition which become noticeable at $T \gtrsim 1$ MeV. We find that the isospin relaxation rate rises rapidly as temperature rises, and at $T \approx 5$ MeV it is comparable to the timescale of the density oscillations that occur immediately after the merger. This produces a resonant peak in the bulk viscosity at $T \approx 5$ MeV, which causes density oscillations to be damped on the timescale of the merger. Our calculations suggest that isospin relaxation dynamics may also be relevant when neutrinos are treated more accurately via neutrino transport schemes.

DOI: 10.1103/PhysRevC.109.055803

I. INTRODUCTION

Nuclear matter in neutron stars relaxes towards isospin ("beta") equilibrium; its steady state has an equilibrium proton fraction $x_p^{\rm eq}$ which is a function of baryon density n_B and temperature T. Equilibrium is established by weak interactions which operate on a timescale that can range from microseconds to minutes. Astrophysical phenomena such as density oscillations in neutron stars, which can be on a similar timescale, can therefore drive the system out of equilibrium, and the dynamics of the relaxation process may be relevant to our understanding of the astrophysics.

In this analysis we focus on the astrophysical conditions found in the central region of neutron star mergers, where homogeneous nuclear matter at densities from one to several times nuclear saturation density n_0 and temperatures up to 80 MeV undergoes compression and rarefaction on millisecond timescales [1,2]. The purpose of this work is to argue that such oscillations are likely to drive the system out of isospin equilibrium [3], and that it is important for simulations to track its relaxation back to chemical equilibrium, using the most accurate available Urca rate calculations, because it may lead to physically important phenomena such as bulk viscosity.

A major complication is the role of neutrinos. There are two limits in which they can be straightforwardly handled. The first is the "neutrinoless" limit where the contribution to flavor equilibration from neutrino absorption is negligible. This can be due to there being few neutrinos present and/or to their having a low absorption cross section, e.g., at low temperatures. The second is the "neutrino-trapped" regime where neutrinos have a short mean free path, e.g., at high temperatures, and hence form a locally equilibrated Fermi gas. In general, neutrinos in the central region of a merger are expected to lie between these two extremes, and techniques are still being developed to handle their complex dynamics [4,5].

In neutrino-trapped matter, isospin equilibration proceeds so fast that the relaxation dynamics can be neglected [6–8], but previous work on neutrinoless matter found that isospin relaxation occurs on the same timescale as the fluid dynamics, giving rise to maximal bulk viscosity [9–12]. This paper focuses on the neutrinoless regime, and provides an improved treatment in various respects (see summary below) that aims to reinforce the earlier conclusions, namely, that since isospin relaxation dynamics are important in one of the two extreme limits, there is good reason to do the best possible job of including them in more realistic neutrino transport schemes. In the Conclusions we outline our future plans towards this goal.

Given this motivation, we calculate physical quantities relevant for isospin equilibration in neutrinoless homogeneous nuclear matter at densities above nuclear saturation density. We focus our calculation on the range $0 < T < 10$ MeV because neutrino trapping becomes stronger as temperatures rise beyond a few MeV [13]. At these temperatures we can neglect positrons because at the densities we study the electron chemical potential μ_e is in the 100 MeV range so $T \ll \mu_e$. We neglect muons because they introduce extra processes requiring a more sophisticated treatment. Previous analyses have found that they do not make a large difference to the equilibration and relaxation rates [14], so we postpone their inclusion to future work. The quantities we calculate are the isospin relaxation rate γ_I and the the frequency-dependent bulk viscosity ζ and damping (sound attenuation) time for density oscillations.

Previous work on isospin relaxation in neutrinoless matter has assumed that the condition for isospin equilibrium is

*alford@wustl.edu

†ahaber@physics.wustl.edu

‡ziyuan.z@wustl.edu

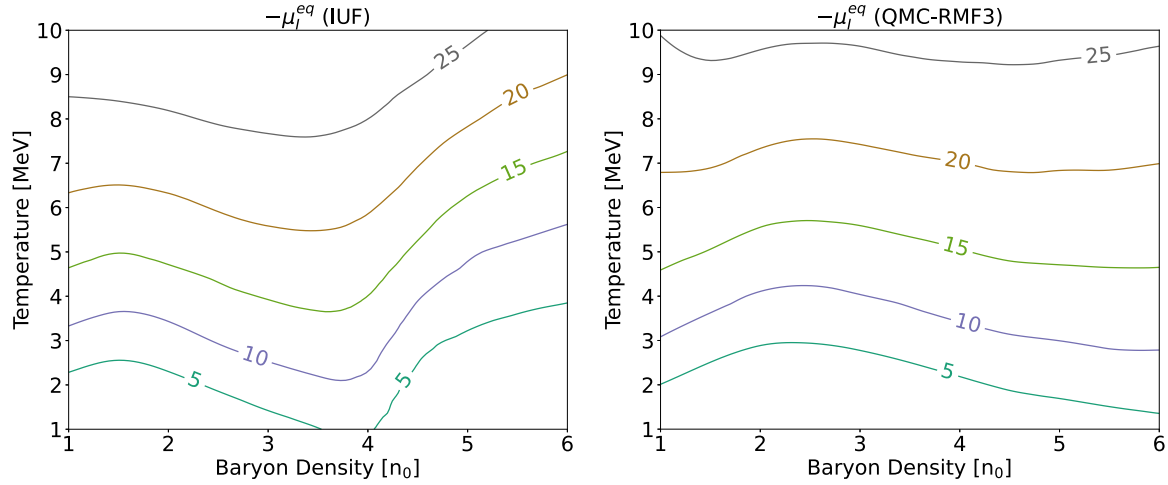

FIG. 1. Density and temperature dependence of $-\mu_I^{\rm eq}$, the isospin chemical potential in isospin equilibrium [Eq. (1)], for the IUF equation of state (left panel) and QMC-RMF3 (right panel); $-\mu_I^{\rm eq}$ rises with temperature because it arises from thermal blurring of the Fermi surfaces (see text). For IUF at low temperatures it is also influenced by the direct Urca threshold at $n_B \approx 4n_0$.

$\mu_n = \mu_p + \mu_e$ (e.g., [9,12,15–22]). As we will now discuss, this is only valid at temperatures below about 1 MeV. At the temperatures attained in neutron star mergers there is a non-negligible correction to this condition. In this paper, we calculate the isospin relaxation rate and bulk viscosity using the proper equilibrium condition.

In the infinite volume thermodynamic limit, equilibrium is established when the forward and backward rates of each process are equal ("detailed balance"), so the equilibrium condition is a simple equality involving chemical potentials. However, neutrino transparency is a finite-volume effect, arising when the mean free path of neutrinos is not much smaller than the size of the system. In a neutrinoless system neutrinos only occur in final states, never in initial states, so the system does not obey the principle of detailed balance. Equilibrium is attained when there is a balance between *different* processes: neutron decay and electron capture [as seen in Eqs. (24) and (25) below]. In general, the equilibrium condition in neutrinoless matter takes the form [10,13]

$$\mu_n = \mu_p + \mu_e - \mu_I^{\rm eq}(n_B, T), \tag{1}$$

where there is an isospin chemical potential $\mu_I^{\rm eq}$ whose value is determined by the requirement that the net rate of isospin creation is zero, i.e., the neutron decay and electron capture rates (26) are equal,

$$\Gamma_I \equiv \Gamma^{\rm net}_{n\to p} = 0. \tag{2}$$

At sufficiently low temperatures, $T \ll 1$ MeV, the correction $\mu_I^{\rm eq}$ in Eq. (1) becomes negligible because the Fermi surface approximation is valid: the Fermi-Dirac distribution exponentially suppresses contributions from particles away from their Fermi surfaces and the energy carried away by neutrinos is negligible (of order T). If neutrinos are kinematically negligible then neutron decay and electron capture are effectively the time-reverse of each other, $n \leftrightharpoons p\, e^-$, and the isospin equilibrium condition can be obtained from applying detailed balance to that process, yielding $\mu_n = \mu_p + \mu_e$, i.e., $\mu_I^{\rm eq} = 0$. However, as the temperature rises above about 1 MeV, $\mu_I^{\rm eq}$ becomes non-negligible, and can reach values as large as 20 MeV (see Fig. 1 and Refs. [10,13]).

In Sec. II we derive expressions for the isospin relaxation rate and the bulk viscosity in terms of the microscopic isospin equilibration rate Γ_I, i.e., the rate of Urca processes. In Sec. III we describe the relativistic mean field theories (RMFTs) that we use to model nuclear matter. In Sec. IV we summarize the calculation of the Urca rates and in Sec. V we present our results.

We use natural units where $\hbar = c = k_B = 1$.

II. ISOSPIN EQUILIBRATION OF NUCLEAR MATTER

We now derive expressions for the isospin relaxation rate γ_I and the bulk viscosity ζ of neutrinoless npe matter at arbitrary temperature. We will assume that matter always remains locally electrically neutral, so all calculations are performed at constant charge density $n_Q = 0$. The derivation in this section is applicable to both isothermal and adiabatic density oscillations, by taking the derivatives at constant temperature or constant entropy per baryon, respectively. In the presentation below we will not explicitly show the dependence on T or s/n_B.

A. Isospin relaxation

In neutrinoless nuclear $npe(\mu)$ matter, in addition to the conserved baryon number B and conserved electric charge Q there is another "briefly conserved" charge, isospin I. The relevant charge densities and chemical potentials can be related to the net densities and chemical potentials of neutrons (n), protons (p), and electrons (e),

$$\begin{aligned} n_B &= n_p + n_n, \\ n_I &= \tfrac{1}{2}n_p - \tfrac{1}{2}n_n, \\ n_Q &= n_p - n_e, \\ \mu_B &= \tfrac{1}{2}\mu_p + \tfrac{1}{2}\mu_n + \tfrac{1}{2}\mu_e, \end{aligned}$$

$$\mu_I = \mu_p - \mu_n + \mu_e,$$
$$\mu_Q = -\mu_e. \tag{3}$$

The expressions above do not include a chemical potential for lepton number because the neutrinos are far from thermal equilibrium so there is no associated chemical potential.

It will be convenient to define the isospin fraction x_I, which is simply related to the proton fraction ($x_p \equiv n_p/n_B$),

$$x_I \equiv \frac{n_I}{n_B} = x_p - \frac{1}{2}. \tag{4}$$

For many purposes we can treat x_I as equivalent to x_p, since $\partial/\partial x_I$ is the same as $\partial/\partial x_p$, and a derivative at constant x_I is also a derivative at constant x_p.

As noted in Sec. I, on strong-interaction ($\approx 10^{-23}$ s) timescales all three charges are conserved, but on longer timescales the weak interactions break isospin, so μ_I and x_I relax to their β equilibrated values $\mu_I^{\rm eq}$ and $x_I^{\rm eq}$. To analyze this equilibration process, where the system has been driven out of equilibrium by a density oscillation, it is natural to work in terms of n_B and x_I, since baryon density is the quantity that tracks the density oscillation, and the isospin fraction tracks relaxation to equilibrium.

Equilibration of isospin is governed by the rate equation

$$\frac{dn_I}{dt} = \frac{n_I}{n_B}\frac{dn_B}{dt} + \Gamma_I(n_B, x_I). \tag{5}$$

The first term on the right side tells us that if isospin were conserved then compression would change the isospin density by the same fraction as it changes baryon density. In the second term Γ_I is the *isospin production rate*, i.e., the net rate per unit volume at which isospin increases, or equivalently the net rate at which neutrons are converted to protons. In Sec. IV we describe how it can be calculated from the Fermi theory of weak interactions by integrating the net $n \to p$ rate over the Fermi-Dirac distributions of protons, neutrons, and electrons.

Using the definition (4), the rate equation (5) becomes

$$\frac{dx_I}{dt} = \frac{1}{n_B}\Gamma_I(n_B, x_I), \tag{6}$$

and the equilibrium isospin fraction $x_I^{\rm eq}(n_B)$ is defined by

$$\Gamma_I\big(n_B, x_I^{\rm eq}(n_B, T)\big) = 0. \tag{7}$$

If x_I is above its equilibrium value then there are too many protons, so the rate of $p \to n$ becomes larger than $n \to p$; Γ_I should then become negative, driving x_I back down towards its equilibrium value. To obtain physically relevant quantities such as the isospin relaxation rate and bulk viscosity we consider a generic small departure from equilibrium,

$$\Gamma_I(\bar{n}_B + \Delta n_B, \bar{x}_I + \Delta x_I) = \left.\frac{\partial \Gamma_I}{\partial n_B}\right|_{x_I} \Delta n_B + \left.\frac{\partial \Gamma_I}{\partial x_I}\right|_{n_B} \Delta x_I, \tag{8}$$

where $\bar{x}_I \equiv x_I^{\rm eq}(n_B)$. Using this in the rate equation (6) we obtain the rate equation for the isospin fraction

$$\frac{dx_I}{dt} = -\gamma_I \Delta x_I + \gamma_B \frac{\Delta n_B}{\bar{n}_B}, \tag{9}$$

where

$$\gamma_I \equiv -\frac{1}{\bar{n}_B}\left.\frac{\partial \Gamma_I}{\partial x_I}\right|_{n_B},$$
$$\gamma_B \equiv \left.\frac{\partial \Gamma_I}{\partial n_B}\right|_{x_I}, \tag{10}$$

with both the derivatives evaluated at $n_B = \bar{n}_B$, $x_I = \bar{x}_I$. According to Eq. (9) a small deviation of x_I from equilibrium (with no change in n_B) would evolve as $\dot{x}_I = -\gamma_I(x_I - x_I^{\rm eq})$, so we identify γ_I as the *isospin relaxation rate*, which we expect to be positive.

The other rate factor, γ_B, tells us how quickly equilibrium is restored in response to a change in density at fixed isospin fraction. In previous treatments (e.g., [15–22]) this was simply related to γ_I [see Eq. (A4)] because it was assumed that β equilibrium corresponds to $\mu_I = 0$; however, as noted in Sec. I, this is no longer true if the neutrinos are out of thermal equilibrium at $T \gtrsim 1$ MeV.

B. Bulk viscosity

To see how isospin equilibration leads to bulk viscous damping, we consider a fluid element of nuclear matter, with pressure p, that is driven out of equilibrium by a small-amplitude density oscillation,

$$n_B(t) = \bar{n}_B + \mathrm{Re}(\delta n_B\, e^{i\omega t}),$$
$$x_I(t) = \bar{x}_I + \mathrm{Re}(\delta x_I\, e^{i\omega t}),$$
$$p(t) = \bar{p} + \mathrm{Re}(\delta p\, e^{i\omega t}). \tag{11}$$

We assume that the oscillation occurs around equilibrium, so

$$\bar{x}_I = x_I^{\rm eq}(\bar{n}_B, T). \tag{12}$$

We adopt the phase convention that the baryon density amplitude $\delta n_B \ll \bar{n}_B$ is real. Bulk viscous dissipation arises from a phase lag between pressure and density. The rate of energy dissipation for the small-amplitude oscillation (11) is obtained from the pdV work done by the oscillation in one cycle. Rewriting pdV as $p\,(dV/dt)\,dt$ the rate of energy dissipation per unit volume is

$$W = -\frac{1}{\tau \bar{V}}\int_0^\tau p(t)\frac{dV}{dt}dt = \frac{1}{2}\omega\,\mathrm{Im}(\delta p)\,\frac{\delta n_B}{\bar{n}_B}, \tag{13}$$

where the period is $\tau = 2\pi/\omega$ and we used Eq. (11) and the relation $n_B = N/V$ for a fluid element containing N baryons.

The hydrodynamic relation between bulk viscosity and rate of energy dissipation per unit volume is $W = \zeta(\nabla \cdot \vec{v})^2$, which for the small-amplitude oscillation (11) becomes (averaged over one oscillation period)

$$W = \frac{1}{2}\zeta\omega^2\frac{(\delta n_B)^2}{\bar{n}_B^2}. \tag{14}$$

Identifying Eq. (13) with Eq. (14) we obtain the frequency-dependent bulk viscosity

$$\zeta(\omega) = \frac{\mathrm{Im}(\delta p)}{\delta n_B}\frac{\bar{n}_B}{\omega}. \tag{15}$$

For *npe* nuclear matter, where the phase lag of the pressure arises from the equilibration of isospin, this becomes

$$\zeta(\omega) = \frac{\bar{n}_B}{\omega} \left.\frac{\partial p}{\partial x_I}\right|_{n_B} \frac{\mathrm{Im}(\delta x_I)}{\delta n_B}. \tag{16}$$

We can now obtain the bulk viscosity of nuclear matter by analyzing the equilibration process in more detail, which will allow us to calculate the phase lag. Substituting the explicit form of the oscillations (11) in to the rate equation (9) we find the relationship between the amplitudes δx_I and δn_B

$$i\omega \delta x_I = -\gamma_I \delta x_I + \frac{\gamma_B}{\bar{n}_B} \delta n_B, \tag{17}$$

which can be rewritten

$$\frac{\delta x_I}{\delta n_B} = \frac{1}{\bar{n}_B} \frac{\gamma_B}{\gamma_I + i\omega}. \tag{18}$$

For the bulk viscosity (16) we take the imaginary part of Eq. (18),

$$\zeta = -\left.\frac{\partial p}{\partial x_I}\right|_{n_B} \frac{\gamma_B}{\gamma_I^2 + \omega^2}, \tag{19}$$

where γ_B and γ_I are defined in Eq. (10) This is the general expression for the bulk viscosity, valid even when temperature corrections shift the equilibrium away from its low temperature limit $\mu_I^{\rm eq} = 0$. In Appendix A we take the low temperature limit and show that previous calculations, which assumed $\mu_I^{\rm eq} = 0$, agree with the general result in that limit. In the low temperature limit (A5) it is clear that the dependence of bulk viscosity on density and temperature features a resonant maximum when the relaxation rate $\gamma_I(n_B, T)$ coincides with the angular frequency ω of the density oscillation. This is less clear in the more general expression (19), but we have found that for typical equations of state $\mu_I^{\rm eq}$ varies slowly enough as a function of n_B and T so that $\gamma_B(n_B, T)$ is still roughly proportional to $\gamma_I(n_B, T)$ (the constant of proportionality is a slowly varying function of n_B and T), so the resonant peak is still present.

The bulk viscosity (19) can also be written as

$$\zeta = \zeta_0 \frac{\gamma_I^2}{\gamma_I^2 + \omega^2}, \tag{20}$$

where

$$\zeta_0 = -\left.\frac{\partial p}{\partial x_I}\right|_{n_B} \frac{\gamma_B}{\gamma_I^2} \tag{21}$$

is the static (zero frequency) limit of the bulk viscosity. (Note that in the isothermal regime the derivative of the pressure can be rewritten as a derivative of μ_I, see Appendix B). From the static bulk viscosity and the isospin relaxation rate γ_I, which are functions of n_B and T, one can reconstruct the full frequency-dependent bulk viscosity as a function of density and temperature.

III. NUCLEAR MATTER MODELS

One of the most important features influencing the isospin relaxation rate of nuclear matter is the direct Urca threshold density, which separates the low-density range, where in the $T \to 0$ limit only modified Urca processes are allowed, from the high-density range where direct Urca processes are kinematically allowed (see Sec. IV). It is not known whether real-world nuclear matter has a direct Urca threshold in the relevant density range, so we perform calculations for two relativistic mean-field theories, IUF [23] and QMC-RMF3 [24]. Both are consistent with current astrophysical and nuclear constraints. IUF has a direct Urca threshold at $4\,n_0$ whereas QMC-RMF3 does not have a threshold in the range of densities found in neutron stars.

At a given baryon density n_B, temperature T, and proton fraction x_p we solve the RMFT mean field equations to obtain the values of the meson condensates, thermodynamic quantities such as the pressure and proton and neutron chemical potentials, and also the nucleon effective masses and energy shifts. The dispersion relations for nucleons in the relativistic mean field models are then specified as

$$E_n = \sqrt{m_n^{*2} + k_n^2} + U_n, \tag{22}$$

$$E_p = \sqrt{m_p^{*2} + k_p^2} + U_p, \tag{23}$$

where m_i^* are the effective masses, k_i are the particle momenta, and U_i are the energy shifts. In RMFTs the effective masses and energy shifts are functions of density, temperature, and proton fraction. In the models that we use the protons and neutrons have the same effective mass, so the energy shifts play an important role by separating the neutron and proton energies and thereby opening up more phase space for the Urca processes.

IV. URCA RATES

A. Overview of Urca processes

The isospin equilibration rate Γ_I Eq. (5) is given by the neutron decay and electron capture processes, which are governed by the weak interaction. Depending on the number of spectators, these processes are called direct or modified Urca. The direct Urca processes in neutrino transparent matter are neutron decay and electron capture

$$n \to p + e^- + \bar{\nu}, \quad p + e^- \to n + \nu. \tag{24}$$

In most models of homogeneous nuclear matter the proton fraction x_p increases monotonically with the density. This means that for some models there is a direct Urca threshold density, defined as the density below which, in the limit $T \to 0$, the rate of the direct Urca process is exponentially suppressed. Since at low temperature the participating neutrons, protons, and electrons are all on their Fermi surfaces, the criterion for direct Urca to proceed is $k_{Fn} \leqslant k_{Fp} + k_{Fe}$ where k_{Fi} are the Fermi momenta for the particles. In *npe* matter this threshold is $x_p \geqslant 0.11$ since neutrality requires $k_{Fp} = k_{Fe}$. Below the threshold density, $k_{Fn} > k_{Fp} + k_{Fe}$, so momentum conservation forbids the direct Urca processes for particles on their Fermi surfaces. In order for momentum conservation to be satisfied, some particles would need to be away from their Fermi surfaces, but this population is exponentially suppressed by their Fermi-Dirac distributions. Consequently, the direct Urca rate is suppressed as $\exp(-\mathcal{E}/T)$ where $\mathcal{E}$

is an energy deficit that goes to zero as the density reaches the dUrca threshold from below. At densities below the direct Urca threshold (and temperatures well below the energy deficit for the given density) we expect the Urca rates to be dominated by the modified Urca process,

$$\begin{aligned} N + n &\to N + p + e^- + \bar{\nu}, \\ N + p + e^- &\to N + n + \nu, \end{aligned} \tag{25}$$

where N is a spectator nucleon that can scatter from one part of its Fermi surface to another, injecting momentum via a virtual pion in to the accompanying direct Urca process.

We now discuss the calculation of the direct Urca ("dU") and modified Urca ("mU") rates, which establish β equilibrium (see Sec. II),

$$\Gamma_{\rm nd} = \Gamma_{\rm dU,nd} + \Gamma_{\rm mU,nd}, \tag{26}$$

$$\Gamma_{\rm ec} = \Gamma_{\rm dU,ec} + \Gamma_{\rm mU,ec}. \tag{27}$$

In this paper, we will calculate the direct Urca rates by integrating over the full phase space, including Fermi-Dirac-suppressed contributions that become non-negligible when the temperature rises to the MeV range [13]. We will calculate modified Urca rates in the Fermi surface approximation (in which participating nucleons and electrons are assumed to be on their Fermi surfaces) since modified Urca always has a nonsuppressed contribution from such particles.

B. Direct Urca rates

The direct Urca neutron decay and electron captures rates are [25]

$$\begin{aligned} \Gamma_{\rm nd} = \int & \frac{d^3k_n}{(2\pi)^3}\frac{d^3k_p}{(2\pi)^3}\frac{d^3k_e}{(2\pi)^3}\frac{d^3k_\nu}{(2\pi)^3} \\ & \times f_n(1-f_p)(1-f_e)\frac{\sum|M|^2}{(2E_n^*)(2E_p^*)(2E_e)(2E_\nu)} \\ & \times (2\pi)^4\delta^{(4)}(k_n - k_p - k_e - k_\nu), \end{aligned} \tag{28}$$

and

$$\begin{aligned} \Gamma_{\rm ec} = \int & \frac{d^3k_n}{(2\pi)^3}\frac{d^3k_p}{(2\pi)^3}\frac{d^3k_e}{(2\pi)^3}\frac{d^3k_\nu}{(2\pi)^3} \\ & \times (1-f_n)f_p f_e\frac{\sum|M|^2}{(2E_n^*)(2E_p^*)(2E_e)(2E_\nu)} \\ & \times (2\pi)^4\delta^{(4)}(k_p + k_e - k_n - k_\nu), \end{aligned} \tag{29}$$

where $\Sigma|M|$ is the spin-summed matrix element, $E_i^* = \sqrt{k_i^2 + m_i^{*2}}$ are the effective nucleon dispersion relations, $E_e = \sqrt{k_e^2 + m_e^2}$ and $E_\nu = k_\nu$ are the electron/neutrino dispersion relations, and f_i are Fermi-Dirac distributions. Direct Urca rates are often calculated in various approximations such as using nonrelativistic dispersion relations for the nucleons [6,13,17,22], using vacuum masses for the nucleons [13], simplifying the matrix element [6,22], or using the Fermi surface approximation [17].

Our direct Urca rate calculations use the complete matrix element, relativistic dispersion relations for all participating particles, and integrate momenta over the entire phase space. For details see Appendix A of Ref. [10].

C. Modified Urca rates

We use the standard expressions for the modified-Urca neutron decay and electron captures rates,

$$\begin{aligned} \Gamma_{mU,nd} = \int & \frac{d^3k_n}{(2\pi)^3}\frac{d^3k_p}{(2\pi)^3}\frac{d^3k_e}{(2\pi)^3}\frac{d^3k_\nu}{(2\pi)^3}\frac{d^3k_{N_1}}{(2\pi)^3}\frac{d^3k_{N_2}}{(2\pi)^3} \\ & \times (2\pi)^4\delta^{(4)}(k_n + k_{N_1} - k_p - k_e - k_\nu - k_{N_2}) \\ & \times f_n f_{N_1}(1-f_p)(1-f_e)(1-f_{N_2}) \\ & \times \left(s\frac{\sum|M|^2}{2^6E_n^*E_p^*E_eE_\nu E_{N_1}^*E_{N_2}^*}\right) \end{aligned} \tag{30}$$

and

$$\begin{aligned} \Gamma_{mU,ec} = \int & \frac{d^3k_n}{(2\pi)^3}\frac{d^3k_p}{(2\pi)^3}\frac{d^3k_e}{(2\pi)^3}\frac{d^3k_\nu}{(2\pi)^3}\frac{d^3k_{N_1}}{(2\pi)^3}\frac{d^3k_{N_2}}{(2\pi)^3} \\ & \times (2\pi)^4\delta^{(4)}(k_p + k_e + k_{N_1} - k_n - k_\nu - k_{N_2}) \\ & \times f_p f_e f_{N_1}(1-f_n)(1-f_{N_2}) \\ & \times \left(s\frac{\sum|M|^2}{2^6E_n^*E_p^*E_eE_\nu E_{N_1}^*E_{N_2}^*}\right), \end{aligned} \tag{31}$$

where $s = 1/2$ is a symmetry factor to account for identical particles. These are obtained using the matrix element from Refs. [26,27] and using the Fermi surface approximation to simplify the phase space integral. For details see Appendix B of [10].

V. RESULTS

We now present numerical results for the quantities described in Sec. II. We perform all the computations in the isothermal regime: see Sec. VI for further discussion of this assumption.

A. Isospin chemical potential

To calculate linear-response isospin equilibration properties such as the relaxation rate or bulk viscosity one needs to perturb around the equilibrium state, i.e., the state in which the net rate of isospin creation is zero. As noted in Sec. I, at nonzero temperature this requires a nonzero isospin chemical potential, $\mu_I^{\rm eq}$ [Eq. (1)]. Its value is negative because thermal corrections enhance electron capture more than neutron decay, so to restore the balance between these rates we need a chemical potential that reduces the proton fraction: this suppresses electron capture by reducing the proton population and enhances neutron decay by adding more occupied neutron states.

In Fig. 1 we show how $-\mu_I^{\rm eq}$ varies with density and temperature for our two exemplary equations of state, IUF and QMC-RMF3. The plot shows contours labeled by their value of $-\mu_I^{\rm eq}$. As discussed in Refs. [10,13] $\mu_I^{\rm eq}$ tends to zero as $T \to 0$ which is why it was neglected in previous treatments of bulk viscosity in neutron stars. However, as the temperature

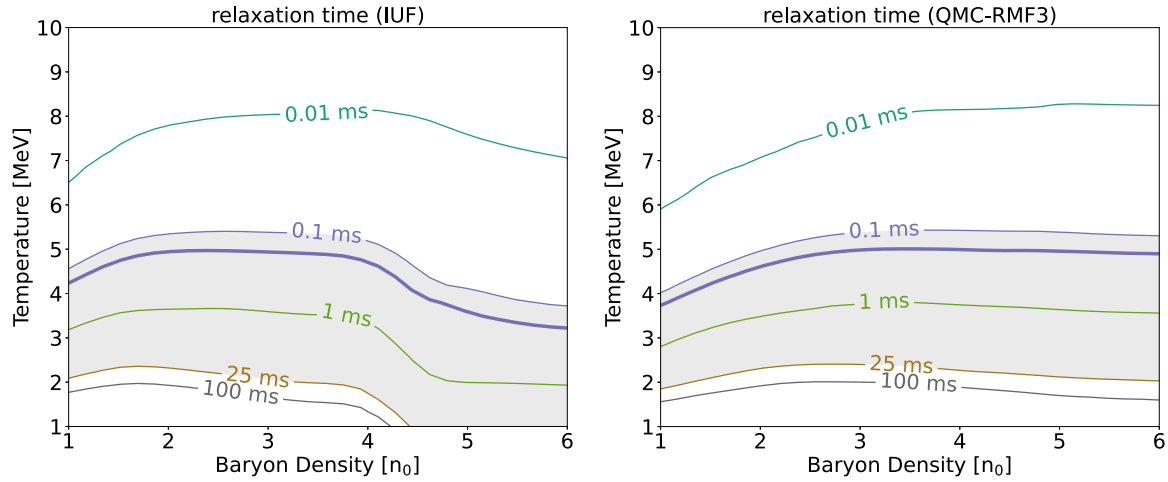

FIG. 2. Density and temperature dependence of the isospin relaxation time $\tau = 1/\gamma_I$ [Eq. (10)]. The shaded region shows where the relaxation time is between 0.1 ms and 25 ms, i.e., comparable to the timescale of merger dynamics. The thick line shows the temperatures and densities where the bulk viscosity of a 1 kHz density oscillation would reach its maximum, i.e., where $\gamma_I = 2\pi \times 1\,\text{kHz}$ (Sec. II B).

rises above about 1 MeV, it becomes non-negligible. Note that for IUF, which has a direct Urca threshold at $n_B \approx 4n_0$, μ_I^{eq} is enhanced near the threshold density. This is because thermal blurring of the Fermi surfaces becomes more important close to threshold, and opens up phase space for the electron capture process more than it does for neutron decay [10,13]; this imbalance is the reason for a nonzero μ_I^{eq}.

B. Isospin relaxation rate

Figure 2 shows how the isospin relaxation time $\tau = 1/\gamma_I$ (10) depends on density and temperature for our two reference equations of state, IUF (left) and QMC-RMF3 (right). We have shaded the range of density and temperature where relaxation occurs on the timescale relevant for mergers, 0.1 ms to 25 ms. The thick contour shows where $\gamma_I = 2\pi \times 1\,\text{kHz}$, which as we will see below is where the bulk viscosity reaches a resonant maximum for a 1 kHz oscillation. If there is material in a merger that lies in this density and temperature range and obeys our assumptions (such as neutrino transparency), then the relaxation of its proton fraction occurs on a timescale that is comparable to that of the merger dynamics, indicating that the relaxation process should be included in simulations.

In regions where the equilibration time is much smaller than 0.1 ms equilibration happens so fast that one could use the approximation that the matter is always in isospin equilibrium. In regions where the equilibration time is much longer than 20 ms the equilibration process is slow, and the proton fraction of each fluid element could be approximated as being constant. Previous simulations of neutron star mergers have either investigated these extreme cases of instantaneous equilibration, or frozen composition [28] or only partly implemented the low density and low-temperature approximation to the Urca rates studied here [5,29–32].

Recently a first attempt has been made [11] to include both direct and modified Urca processes, calculated in the Fermi surface approximation, in the simulation. It was found that Urca processes affect the proton fraction of the fluid elements on the timescale of the merger dynamics.

For the IUF equation of state there is a noticeable feature in the relaxation time plot: relaxation becomes faster when the density reaches around $4n_0$. This is because IUF has a direct Urca threshold at this density. At densities above this threshold more phase space opens up and Urca rates, at a given temperature, are much faster than they are at densities below the threshold. Below the threshold density, the relaxation time is comparable to the merger timescale at temperatures of order 2 to 4 MeV. Above the threshold density, the relaxation time is comparable to the merger timescale at temperatures below 2 MeV.

For QMC-RMF3, the relaxation time depends only weakly on density. This is because there is no direct Urca threshold. Across the whole density range that we studied β equilibrium is determined by a balance between neutron decay (dominated by modified Urca) and electron capture (dominated by direct Urca) [10,13]. Consequently, the region where the relaxation time is comparable to the merger timescale extends across the whole density range that we computed, for temperatures in the MeV-range.

Assuming that our reference equations of state (EOSs) are representative, Fig. 2 implies that if neutrinoless homogeneous matter is present in mergers then regions at $T \lesssim 5\,\text{MeV}$ will likely be driven out of isospin equilibrium and regions at $T \approx 2$ to 5 MeV (the exact range depending on the EoS) will equilibrate on the timescale of the merger.

C. Bulk viscosity and damping time

In Fig. 3 we show the density and temperature dependence of the static (zero-frequency) bulk viscosity ζ_0 Eq. (21). The plot shows contours of $\log_{10}(\zeta_0)$ where ζ_0 is in cgs units ($\text{g cm}^{-1}\,\text{s}^{-1}$). The static bulk viscosity depends inversely on the relaxation rate, so it drops as the temperature rises, and at low temperatures we also see the effects of the direct Urca threshold at $n_B \approx 4n_0$, as in Fig. 2.

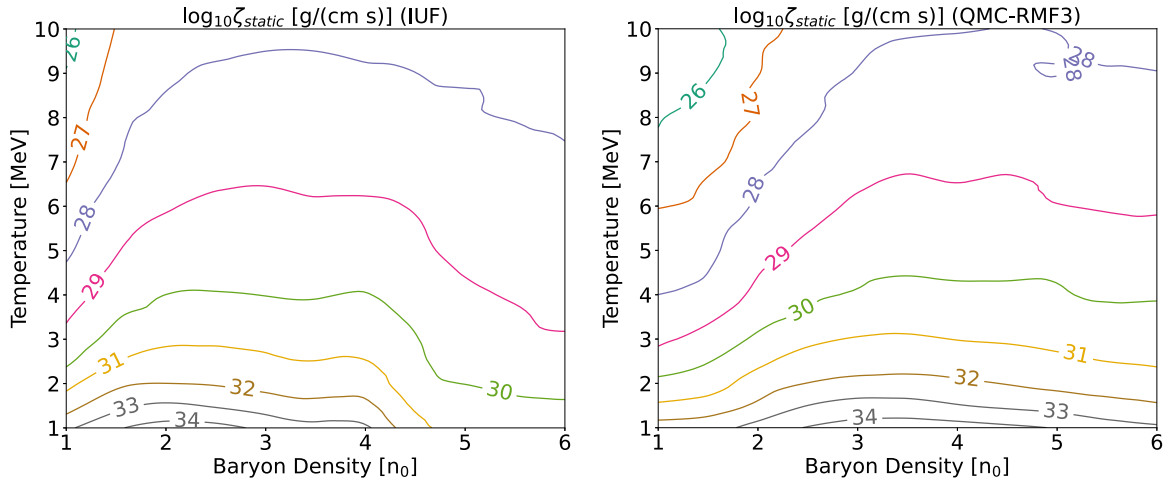

FIG. 3. Static (zero-frequency) bulk viscosity (21) for the IUF (left) and QMC-RMF3 (right) equations of state. The static bulk viscosity drops as temperature rises because it is inversely proportional to the relaxation rate.

From the isospin relaxation rate and the static bulk viscosity one can reconstruct the frequency-dependent bulk viscosity [Eq. (20)]. Since density oscillations in neutron star mergers typically have frequencies in the kHz range, Fig. 4 shows the density and temperature dependence of bulk viscosity at angular frequency $\omega = 2\pi \times$ kHz.

As described in Sec. II B, we expect the bulk viscosity to reach a resonant maximum when the isospin relaxation rate $\gamma_I(n_B, T)$ coincides with the angular frequency ω of the density oscillation. The relaxation rate rises quickly with temperature since higher temperature opens up more phase space near the Fermi surfaces. We therefore expect the bulk viscosity to achieve its maximum value at the temperature where $\gamma_I(n_B, T) \approx \omega$. From Fig. 2 we see that for a 1 kHz density oscillation that temperature is around 5 MeV. This explains what we see in Fig. 4: the contours run roughly horizontally, with the bulk viscosity reaching a maximum at $T \approx 5$ MeV. At lower temperatures the system equilibrates so slowly that isospin is almost conserved: the proton fraction remains constant, and the system has a low bulk viscosity. At higher temperatures where $\gamma_I \gg \omega$ the system equilibrates so quickly that there is little phase lag between pressure and density, and the bulk viscosity tends towards its static value ζ_0 [Eq. (21)].

For the IUF EoS one can see the effect of the direct Urca threshold at $n_B \approx 4n_0$: below that density relaxation is slower (due to a lack of kinematically allowed phase space), and so a higher temperature is needed to bring the relaxation rate up to 1 kHz.

Comparing these to previous calculations that used nonrelativistic dispersion relations for the nucleons (e.g., Refs. [22], [9]), our resonance peaks are shifted to slightly higher temperatures for given densities. This is because in our models of nuclear matter the in-medium effective masses of the nucleons are much lower than the vacuum masses so the relativistic corrections are significant, decreasing the Urca rates and relaxation rates [10,14], which means higher temperatures are required to achieve resonance ($\gamma_I = \omega$).

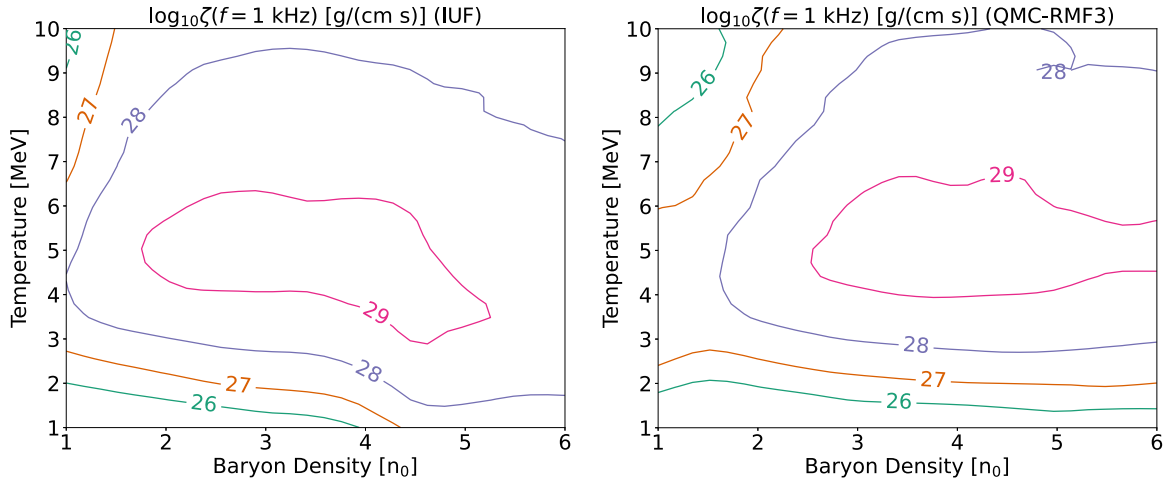

FIG. 4. Bulk viscosity at frequency $f = 1$ kHz for the IUF (left) and QMC-RMF3 (right) equations of state. In both cases the resonant peak occurs where the relaxation rate passes through $\omega = 2\pi \times 1$ kHz, which occurs at $T \approx 5$ MeV.

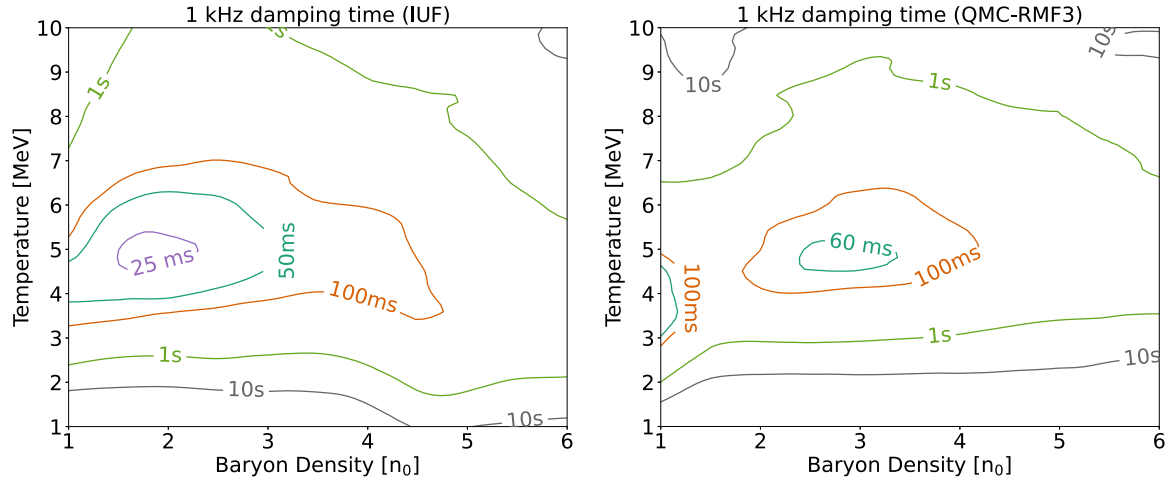

FIG. 5. Damping time for density oscillations of frequency 1 kHz as a function of density and temperature, for the IUF (left) and QMC-RMF3 (right) equations of state.

One physical manifestation of bulk viscosity is the damping of density oscillations. The damping time for an oscillation of angular frequency ω is [9]

$$\tau_{\rm damp} = \frac{\kappa^{-1}}{\omega^2 \zeta(\omega)}, \tag{32}$$

where the incompressibility is

$$\kappa^{-1} \equiv n_B \frac{\partial p}{\partial n_B}\bigg|_{x_I,T}. \tag{33}$$

Since this paper focuses on isothermal density oscillations we use the isothermal compressibility.

Figure 5 shows how the damping time depends on density and temperature for IUF (left) and QMC-RMF3 (right). We expect that in density and temperature regions where the damping time is in the tens of milliseconds range, bulk viscosity will have a significant impact on density oscillations during the merger.

The key features of this plot are:

(1) the temperature dependence of the damping time is mainly determined by that of the bulk viscosity, so the damping time is shortest when the bulk viscosity (Fig. 4) is largest, i.e., at $T \approx 5\,\text{MeV}$;

(2) the density dependence of the damping time also roughly follows that of the bulk viscosity, but damping is slowed at high densities by the growth of the incompressibility: oscillations then store more energy and so take longer to decay;

(3) the shortest damping times are short enough so that bulk viscous damping is relevant on merger timescales.

These results are comparable to those obtained in Ref. [14], which used different models for nuclear matter and used the low-temperature approximation for beta equilibrium, $\mu_I^{\rm eq} = 0$.

The data for the plots shown in this section are available from Ref. [33]. The code used to develop the QMC-RMF3 model and to solve the mean-field equations for both our models of nuclear matter can be found in Ref. [34]. The code for calculating Urca rates and isospin equilibration properties will be made public as part of the MUSES framework [35].

VI. CONCLUSIONS

We have analyzed the isospin equilibration properties of neutrinoless nuclear (npe) matter in the temperature and density range that is relevant to neutron star mergers. Our analysis includes corrections to the isospin equilibrium condition $\mu_n = \mu_p + \mu_e$ which arise at $T \gtrsim 1\,\text{MeV}$. We find that at temperatures of order 2 to 5 MeV the isospin relaxation time, i.e., the timescale on which the proton fraction relaxes to its equilibrium value, is comparable to the timescale of the density oscillations that occur immediately after the merger. At lower temperatures, isospin relaxes more slowly, and at higher temperatures, it relaxes faster. For a 1 kHz density oscillation this leads to a resonant peak in the bulk viscosity at $T \approx 5\,\text{MeV}$, when the relaxation rate matches the frequency. This causes damping of such a density oscillation on the timescale of the merger, providing evidence that when neutrinos are treated more rigorously it may still be important to include isospin relaxation dynamics in merger simulations.

There are many directions in which further work is needed to elucidate the dynamics of isospin under merger conditions:

(1) Our most significant assumption is neutrino transparency, which is valid in the limit of a long mean free path for the neutrinos. The behavior of neutrinos in mergers is more complicated, with an energy-dependent mean free path that interpolates between the transparent and trapped regimes, requiring explicit treatment of neutrino transport [5]. Our next step will be to use the Urca rate calculation methods developed here to provide state-of-the-art calculations of neutrino-energy-dependent rates, suitable for use in transport computations.

(2) Our calculation of the $n \rightleftharpoons p$ rate is based on the standard separation between the direct Urca and modified Urca contributions which are added to give the total rate. Our treatment of direct Urca is full and rigorous, including the

entire weak interaction matrix element and integrating the rate over the whole phase space, but the standard expression for the modified Urca rate uses crude approximations, and improving on it is a natural next step [36].

(3) We performed our calculation in the isothermal regime, assuming that the thermal relaxation rate is faster than the dynamical timescales. It would be straightforward to perform a parallel calculation in the adiabatic regime, but previous analyses [13,14] have found that this does not change the results significantly. This is because the temperatures involved are lower than the Fermi energies of the relevant particles, so the entropy contribution to the pressure is generally a small correction. In reality thermal conduction in mergers is likely to interpolate between the isothermal and adiabatic regimes, again because of the role of neutrinos, which can have a long mean free path depending on their energy and the ambient density and temperature [2], so they likely dominate the thermal conductivity.

(4) Our calculation of bulk viscosity and the damping time for oscillations assumes linear response ("subthermal bulk viscosity") where the amplitude of the oscillations is small in the sense that the departure of the chemical potentials from equilibrium is much less than the temperature. Simulations indicate that in the first few milliseconds after merger there are large-amplitude oscillations, for which the suprathermal bulk viscosity [37,38] would be relevant. We used linear response to obtain suggestive indicators of the potential importance of isospin relaxation dynamics in mergers. As shown in [11], a direct implementation of the Urca rate equation (6) in a merger simulation code will naturally incorporate all physical effects, including the subthermal and suprathermal bulk viscosity.

(5) At merger densities we expect nuclear matter to contain muons, which we neglected in this work. Including them opens up additional equilibration channels ($n \rightleftharpoons p\,\mu$ and purely leptonic processes) leading to a more complicated picture with multiple relaxation times [14].

(6) A natural next step is to compare our results with the isospin equilibration properties of more exotic forms of matter, such as hyperonic [39] or quark matter [20,40–43].

In conclusion, this paper provides the most complete treatment to date of the physics of isospin equilibration in homogeneous neutrinoless nuclear matter, in the density and temperature range that is relevant to neutron star mergers. Our calculation of the isospin relaxation rate and related phenomena such as bulk viscosity and the damping of density oscillations provides a guideline for merger simulators to assess which approximations for isospin equilibration are appropriate at a given density and temperature, and when an explicit implementation of the relaxation process is required.

ACKNOWLEDGMENTS

We thank Liam Brodie for useful discussions. M.G.A. and A.H. are partly supported by the U.S. Department of Energy, Office of Science, Office of Nuclear Physics, under Award No. DE-FG02-05ER41375. Z.Z. is supported in part by the National Science Foundation (NSF) within the framework of the MUSES collaboration, under Grant No. OAC-2103680.

APPENDIX A: COLD β EQUILIBRIUM

Previous calculations of the bulk viscosity of neutrinoless matter assumed that isospin equilibrium occurs when $\mu_n = \mu_p + \mu_e$, i.e., $\mu_I^{\rm eq} = 0$ for any n_B, T. As we have described, this is only valid when the temperature is below about 1 MeV. In this low-temperature regime the isospin creation rate depends only on $\Delta\mu_I$,

$$\Gamma_I = \frac{d\Gamma}{d\mu_I}\Delta\mu_I = \frac{d\Gamma}{d\mu_I}\left(\left.\frac{\partial\mu_I}{\partial x_I}\right|_{n_B}\Delta x_I + \left.\frac{\partial\mu_I}{\partial n_B}\right|_{x_I}\Delta n_B\right). \quad \text{(A1)}$$

To make contact with earlier results we define

$$\chi_{n_B} \equiv -n_B\left.\frac{\partial\mu_I}{\partial n_B}\right|_{x_I} \quad \text{(A2)}$$

and

$$\chi_{x_I} \equiv \frac{1}{\bar{n}_B}\left.\frac{\partial\mu_I}{\partial x_I}\right|_{n_B}. \quad \text{(A3)}$$

Then comparing Eq. (A1) with Eqs. (8) and (9) we can write γ_B in terms of γ_I,

$$\gamma_I = -\chi_{x_I}\frac{d\Gamma}{d\mu_I},$$
$$\gamma_B = \frac{1}{\bar{n}_B}\frac{\chi_{n_B}}{\chi_{x_I}}\gamma_I. \quad \text{(A4)}$$

Using the thermodynamic identity (B1) we can then write the bulk viscosity (20) as

$$\zeta_{\rm cold} = \frac{\chi_{n_B}^2}{\chi_{x_I}}\frac{\gamma_I}{\gamma_I^2+\omega^2}. \quad \text{(A5)}$$

This agrees with previous calculations such as Eq. (128) of Ref. [21].

APPENDIX B: A RELEVANT THERMODYNAMIC IDENTITY

In this Appendix we show that

$$\frac{1}{n_B}\left.\frac{\partial p}{\partial x_I}\right|_{n_B,T} = n_B\left.\frac{\partial\mu_I}{\partial n_B}\right|_{x_I,T}. \quad \text{(B1)}$$

We start by observing that

$$\frac{1}{n_B}\left.\frac{\partial p}{\partial x_I}\right|_{n_B,T} = \left.\frac{\partial p}{\partial n_I}\right|_{n_B,T}. \quad \text{(B2)}$$

Using the thermodynamic expression for pressure, $p = \mu_B n_B + \mu_I n_I + Ts - \varepsilon(n_B, n_I, s)$, and the relation

$$\left.\frac{\partial\varepsilon}{\partial n_I}\right|_{n_B,T} = \left.\frac{\partial\varepsilon}{\partial n_I}\right|_{n_B,s} + \left.\frac{\partial s}{\partial n_I}\right|_{n_B,T}\left.\frac{\partial\varepsilon}{\partial s}\right|_{n_B,n_I}$$
$$= \mu_I + T\left.\frac{\partial s}{\partial n_I}\right|_{n_B,T}, \quad \text{(B3)}$$

it follows that

$$\left.\frac{\partial p}{\partial n_I}\right|_{n_B,T} = n_B\left.\frac{\partial\mu_B}{\partial n_I}\right|_{n_B,T} + n_I\left.\frac{\partial\mu_I}{\partial n_I}\right|_{n_B,T}. \quad \text{(B4)}$$

We now use the Maxwell relation

$$\left.\frac{\partial \mu_B}{\partial n_I}\right|_{n_B,T} = \left.\frac{\partial^2 \varepsilon}{\partial n_B \partial n_I}\right|_T = \left.\frac{\partial \mu_I}{\partial n_B}\right|_{n_I,T}, \tag{B5}$$

where derivatives with respect to n_B are taken at constant n_I and vice versa, so Eq. (B4) becomes

$$\left.\frac{\partial p}{\partial n_I}\right|_{n_B,T} = n_B \left.\frac{\partial \mu_I}{\partial n_B}\right|_{n_I,T} + n_I \left.\frac{\partial \mu_I}{\partial n_I}\right|_{n_B,T} = n_B \left.\frac{\partial \mu_I}{\partial n_B}\right|_{x_I,T}, \tag{B6}$$

which proves Eq. (B2) and therefore Eq. (B1)

[1] L. Baiotti and L. Rezzolla, Binary neutron star mergers: a review of Einstein's richest laboratory, Rep. Prog. Phys. **80**, 096901 (2017).
[2] M. G. Alford, L. Bovard, M. Hanauske, L. Rezzolla, and K. Schwenzer, Viscous dissipation and heat conduction in binary neutron-star mergers, Phys. Rev. Lett. **120**, 041101 (2018).
[3] P. Hammond, I. Hawke, and N. Andersson, Thermal aspects of neutron star mergers, Phys. Rev. D **104**, 103006 (2021).
[4] A. Perego, S. Bernuzzi, and D. Radice, Thermodynamics conditions of matter in neutron star mergers, Eur. Phys. J. A **55**, 124 (2019).
[5] F. Foucart, Neutrino transport in general relativistic neutron star merger simulations, Living Rev. Comput. Astrophys. **9**, 1 (2023).
[6] M. Alford, A. Harutyunyan, and A. Sedrakian, Bulk viscosity of baryonic matter with trapped neutrinos, Phys. Rev. D **100**, 103021 (2019).
[7] M. Alford, A. Harutyunyan, and A. Sedrakian, Bulk viscosity from Urca processes: $npe\mu$ matter in the neutrino-trapped regime, Phys. Rev. D **104**, 103027 (2021).
[8] P. L. Espino, P. Hammond, D. Radice, S. Bernuzzi, R. Gamba, F. Zappa *et al.*, Neutrino trapping and out-of-equilibrium effects in binary neutron star merger remnants, arXiv:2311.00031.
[9] M. G. Alford and S. P. Harris, Damping of density oscillations in neutrino-transparent nuclear matter, Phys. Rev. C **100**, 035803 (2019).
[10] M. G. Alford, A. Haber, S. P. Harris, and Z. Zhang, Beta equilibrium under neutron star merger conditions, Universe **7**, 399 (2021).
[11] E. R. Most, A. Haber, S. P. Harris, Z. Zhang, M. G. Alford, and J. Noronha, Emergence of microphysical viscosity in binary neutron star post-merger dynamics, arXiv:2207.00442.
[12] M. Alford, A. Harutyunyan, and A. Sedrakian, Bulk viscosity from Urca processes: $npe\mu$ matter in the neutrino-transparent regime, Phys. Rev. D **108**, 083019 (2023).
[13] M. G. Alford and S. P. Harris, Beta equilibrium in neutron star mergers, Phys. Rev. C **98**, 065806 (2018).
[14] M. Alford, A. Harutyunyan, and A. Sedrakian, Bulk viscosity of relativistic $npe\mu$ matter in neutron-star mergers, Particles **5**, 361 (2022).
[15] R. F. Sawyer, Bulk viscosity of hot neutron-star matter and the maximum rotation rates of neutron stars, Phys. Rev. D **39**, 3804 (1989).
[16] P. Haensel and R. Schaeffer, Bulk viscosity of hot-neutron-star matter from direct URCA processes, Phys. Rev. D **45**, 4708 (1992).
[17] P. Haensel, K. P. Levenfish, and D. G. Yakovlev, Bulk viscosity in superfluid neutron star cores. I. Direct Urca processes in $npe\mu$ matter, Astron. Astrophys. **357**, 1157 (2000).
[18] P. B. Jones, Bulk viscosity of neutron star matter, Phys. Rev. D **64**, 084003 (2001).
[19] M. E. Gusakov, Bulk viscosity of superfluid neutron stars, Phys. Rev. D **76**, 083001 (2007).
[20] M. G. Alford, S. Mahmoodifar, and K. Schwenzer, Large amplitude behavior of the bulk viscosity of dense matter, J. Phys. G **37**, 125202 (2010).
[21] A. Schmitt and P. Shternin, Reaction rates and transport in neutron stars, Astrophys. Space Sci. Libr. **457**, 455 (2018).
[22] M. Alford, A. Harutyunyan, and A. Sedrakian, Bulk viscous damping of density oscillations in neutron star mergers, Particles **3**, 500 (2020).
[23] F. J. Fattoyev, C. J. Horowitz, J. Piekarewicz, and G. Shen, Relativistic effective interaction for nuclei, giant resonances, and neutron stars, Phys. Rev. C **82**, 055803 (2010).
[24] M. G. Alford, L. Brodie, A. Haber, and I. Tews, Relativistic mean-field theories for neutron-star physics based on chiral effective field theory, Phys. Rev. C **106**, 055804 (2022).
[25] D. G. Yakovlev, A. D. Kaminker, O. Y. Gnedin, and P. Haensel, Neutrino emission from neutron stars, Phys. Rep. **354**, 1 (2001).
[26] B. L. Friman and O. V. Maxwell, Neutron star neutrino emissivities, Astrophys. J. **232**, 541 (1979).
[27] P. Haensel, K. P. Levenfish, and D. G. Yakovlev, Bulk viscosity in superfluid neutron star cores. II. Modified Urca processes in $npe\mu$ matter, Astron. Astrophys. **372**, 130 (2001).
[28] T. Celora, I. Hawke, P. C. Hammond, N. Andersson, and G. L. Comer, Formulating bulk viscosity for neutron star simulations, Phys. Rev. D **105**, 103016 (2022).
[29] M. Ruffert, H. T. Janka, K. Takahashi, and G. Schaefer, Coalescing neutron stars: A step towards physical models. II. Neutrino emission, neutron tori, and gamma-ray bursts, Astron. Astrophys. **319**, 122 (1997).
[30] E. R. Most, L. J. Papenfort, and L. Rezzolla, Beyond second-order convergence in simulations of magnetized binary neutron stars with realistic microphysics, Mon. Not. R. Astron. Soc. **490**, 3588 (2019).
[31] F. Zappa, S. Bernuzzi, D. Radice, and A. Perego, Binary neutron star merger simulations with neutrino transport and turbulent viscosity: impact of different schemes and grid resolution, Mon. Not. Roy. Astron. Soc. **520**, 1481 (2023).
[32] C. Musolino and L. Rezzolla, A practical guide to a moment approach for neutrino transport in numerical relativity, Mon. Not. Roy. Astron. Soc. **528**, 5952 (2024).
[33] https://gitlab.com/ahaber/npe-bulkviscosity.
[34] https://gitlab.com/ahaber.
[35] https://musesframework.io/.
[36] P. S. Shternin, M. Baldo, and P. Haensel, In-medium enhancement of the modified Urca neutrino reaction rates, Phys. Lett. B **786**, 28 (2018).
[37] J. Madsen, Bulk viscosity of strange quark matter, damping of quark star vibration, and the maximum rotation rate of pulsars, Phys. Rev. D **46**, 3290 (1992).
[38] A. Reisenegger and A. Bonacic, Bulk viscosity, *r*-modes, and the early evolution of neutron stars, in *Pulsars, AXPs and SGRs*

observed with BeppoSAX and Other Observatories, Proceedings of the International Workshop held in Marsala, September 23-25, 2002, edited by G. Cusumano, E. Massaro, and T. Mineo (Aracne Editrice, Roma, Italy, 2003), pp. 231–236, arXiv:astro-ph/0303454.

[39] M. G. Alford and A. Haber, Strangeness-changing rates and hyperonic bulk viscosity in neutron star mergers, Phys. Rev. C **103**, 045810 (2021).

[40] M. G. Alford and A. Schmitt, Bulk viscosity in 2SC quark matter, J. Phys. G **34**, 67 (2007).

[41] M. G. Alford, M. Braby, and A. Schmitt, Bulk viscosity in kaon-condensed color-flavor locked quark matter, J. Phys. G **35**, 115007 (2008).

[42] M. Mannarelli and C. Manuel, Bulk viscosities of a cold relativistic superfluid: Color-flavor locked quark matter, Phys. Rev. D **81**, 043002 (2010).

[43] R. Bierkandt and C. Manuel, Bulk viscosity coefficients due to phonons and kaons in superfluid color-flavor locked quark matter, Phys. Rev. D **84**, 023004 (2011).